Article

Structural Studies of Metarhodopsin II, the Activated Form of the G-Protein Coupled Receptor, Rhodopsin

Gregory Choi, Judith Landin, Jhenny Flor Galan, Robert R. Birge, Arlene D. Albert, and Philip L. Yeagle

Biochemistry, **2002**, 41 (23), 7318-7324 • DOI: 10.1021/bi025507w

Structural Studies of Metarhodopsin II, the Activated Form of the G-Protein Coupled Receptor, Rhodopsin†

Gregory Choi, Judith Landin, Jhenny Flor Galan, Robert R. Birge, Arlene D. Albert, and Philip L. Yeagle*

Department of Molecular and Cell Biology, University of Connecticut, Storrs, Connecticut 06269

Received January 7, 2002; Revised Manuscript Received April 9, 2002

ABSTRACT: The structural changes that accompany activation of a G-protein coupled receptor (GPCR) are not well understood. To better understand the activation of rhodopsin, the GPCR responsible for visual transduction, we report studies on the three-dimensional structure for the activated state of this receptor, metarhodopsin II. Differences between the three-dimensional structure of ground state rhodopsin and metarhodopsin II, particularly in the cytoplasmic face of the receptor, suggest how the receptor is activated to couple with transducin. In particular, activation opens a groove on the surface of the receptor that could bind the N-terminal helix of the G protein, transducin α.

Rhodopsin is a member of the large family of G-protein coupled receptors that controls a wide variety of signal transduction systems. The ligand for rhodopsin is retinal, which changes from the 11-cis to the all-trans conformer upon exposure to light. Upon activation of rhodopsin by light, the G-protein, transducin, binds to the cytoplasmic face of rhodopsin and initiates visual signal transduction in the retina. Structures of the cytoplasmic face for both rhodopsin (not activated) and metarhodopsin II (Meta II,[1] the activated form of the receptor) are required to understand this process. A recent X-ray crystallography study, the first three-dimensional structure of any GPCR, revealed many details of the structure of the ground state of bovine rhodopsin but little information about the cytoplasmic face (*1*). There are difficulties that face any attempt at an X-ray crystal structure of Meta II: Meta II is transient, is modulated by the surrounding lipid environment (*2*), and may exist in equilibrium with other forms of the protein (*3*).

Work from many laboratories has shown that the secondary structure of integral membrane proteins built on helical bundles can be defined by the structures of peptides corresponding to helices (*4*−*16*) and turns (*17*−*24*) from those proteins. Recent published results show that these elements of secondary structure can be combined with other experimental, long-range distance constraints to yield a three-dimensional, medium resolution structure of an entire integral membrane protein (*25*). This approach was used to determine the three-dimensional structure of the GPCR, bovine rhodopsin, in its ground state. The structure showed good agreement with the X-ray crystal structure in the transmembrane domain, and in addition provided details of the cytoplasmic face not previously available (*26*).

Here we report studies on the three-dimensional structure of Meta II, utilizing the same approach to membrane protein structure used for that (ground state) rhodopsin structure. The structure obtained for Meta II reveals a conformational change in the receptor upon activation that opens a groove in the surface that is likely involved in binding of the G-protein, transducin.

EXPERIMENTAL METHODS

This study of the structure of Meta II builds on the previous work on the structure of rhodopsin in the ground state. In the study on ground-state rhodopsin, we made the assumption that the secondary structure found in designed peptide segments of the protein reflects the secondary structure in the native protein; in particular, the start and stop points of helices, which residues are in a turn, whether a helix has a break, etc. This assumption was validated for bacteriorhodopsin, which has been studied by both X-ray crystallography and by our approach (*18*, *25*). In those studies, remarkable agreement was observed between the secondary structure in the peptide segments of the protein and the structure of the intact protein by X-ray crystallography.

Therefore, to determine the secondary structure of ground-state rhodopsin, a series of overlapping peptides spanning the rhodopsin sequence was synthesized. Each peptide was designed to contain either a transmembrane helix or a turn of the parent protein. Each peptide sequence overlapped each of its neighbors. Structures of the set of overlapping peptides spanning rhodopsin were determined by two-dimensional homonuclear ^{1}H NMR in solution. Peptides from turns formed turns in solution and peptides from helices showed helices that superimposed on the rhodopsin (ground state) crystal structure (*11*, *12*, *20*, *21*, *27*, *28*).

A construct for the whole protein was assembled from the pieces whose individual structures were determined as described above. The structures in the overlapping sequences of these peptides were superimposed. The construct then consisted of a continuous polypeptide containing the structures of all the peptides with the overlapping sequences.

Both short- and long-range experimental distance constraints were used in the determination of the structure. Short-

† This work was supported by National Institutes of Health Grant EY03328 and R01-GM34548.

* Address correspondence to Philip L. Yeagle. Telephone: 860-486-4363. Fax: 860-486-4331. E-mail: yeagle@uconnvm.uconn.edu.

[1] Abbreviations: Meta II, metarhodopsin II; NMR, nuclear magnetic resonance; PTH, parathyroid hormone.

10.1021/bi025507w CCC: $22.00
Published on Web 05/17/2002

Table 1: Experimental Long-Range Constraints for Rhodopsin[a]

	Meta II (Å)	rhodopsin (Å)
V139C → K248C	23−25	12−14
V139C → E249C	15−20	15−20
V139C → V250C	12−14	15−20
V139C → T251C	23−25	12−14
V139C → R252C	23−25	15−20
H65C → C31 (*29*, *56*, *57*)	12−15	7−10
C140 → S338 (*58*)	15−21	
V204C → F276C (*59*)	2−5	2−5
I251 → V138 (*60*)	<13	
C140 → C222 (*61*)	>7	2−5
C140 → Q225C	2−5	2−5
K245C → Q312C	>7	2−5
R135C → V250C	>7	2−5
K245C → S338C (*62*)	2−5	2−5
S338C → T242C (*63*)	>7	2−5
Y136C → C222	>7	2−5
Y136C → Q225C	2−5	2−5
interhelical distances (*64*)		

[a] About half of the distances in the table are determined from dipolar interactions between two spin labels that are covalently attached to the protein at specific sites (engineered cysteine residues). We use as points of origin for each distance constraint the most distal hydrogens on the native residues at each of the two positions. This employs an approximation that the spin-labeled residue and the nonlabeled native residue point in a similar direction from the protein backbone. Since these cysteine substitutions have little or no effect on protein function according to the published work (see references in Table 1), the assumption just described seems reasonable. However, because of this approximation and possible differences in the length of the normal and modified residues, the distances are converted to range constraints (rather than a specific distance) for use in this structure determination. In the case of disulfides (much of the rest of the list), the distance is defined by the chemistry of the disulfide bond. However, this distance is also converted to a range constraint because the ability to form a disulfide can bridge a wider interresidue gap through thermal motion of the protein than the final chemistry would indicate.

range distance constraints were obtained from the structure determinations of the peptides. All the experimental distance constraints and dihedral angle constraints obtained from the solution structures of each of the peptides were written on the construct (*26*) in a mol2 file with SYBYL (Tripos, St. Louis). Hydrogen bond constraints were added where hydrogen bonds were observed in the original solution structures of the peptides. To define the packing of the secondary structure within the tertiary structure of the protein as described previously (*25*, *26*), long-range distance constraints derived from a variety of independent experiments on intact rhodopsin were added. These experimental constraints are listed in Table 1 and were written into the mol2 file to provide the data with which the resulting structure must satisfy. Simulated annealing produced a structure that satisfied those available experimental data.

The structure obtained for ground-state rhodopsin by this method agreed well with the crystal structure (*26*). The same result had been reported previously for a structure determination of bacteriorhodopsin using the same technique (*25*).

The structural study of Meta II for this report began with the structure of rhodopsin in the ground state obtained as just described. We made one new assumption: that the secondary structure (i.e., start and stop points of helices, which residues defined the turns) does not change as the protein goes from the ground state to metarhodopsin II. The changes in structure between the two forms of the protein are thought to be largely alterations in the spatial relationship of the elements of secondary structure, the helices, and the loops. Previous work on the conformational changes in the activation of rhodopsin was interpreted in terms of rigid body movements of the secondary structures, rather than changes in the extent or location of secondary structure (*29*). This assumption is further encouraged by previous far UV CD spectral data and FTIR data (Katragadda & Albert, unpublished observations) (*30*, *31*) that showed little change in secondary structure between ground state rhodopsin and (bleached) opsin. Recent data from two other proteins also show exclusively rigid body motions upon activation of the membrane protein. CD data on the potassium channel showed no changes in secondary structure upon channel opening, indicating that the changes in conformation must be rigid body motions of existing elements of secondary structure (*32*). CD studies show that conformational changes in the H^+ATPase associated with the changes in state of this membrane enzyme are not accompanied by changes in secondary structure. Substantial rigid body movements, rather than changes in secondary structure, accomplish the conformational changes necessary to cycle through the various states of the enzyme (*33*, *34*). Therefore, all the short-range experimental distance constraints from the NMR data on the peptides that defined the secondary structure of rhodopsin were written into the mol2 file in Sybyl.

A number of experimental long-range distance constraints are available from a variety of studies that describe the spatial relationship of the elements of secondary structure in the Meta II state. Using the data in Table 1, the long-range constraints characterizing ground-state rhodopsin were removed, and the long-range constraints from intact Meta II were written on the ground-state rhodopsin structure. A number of long-range distances between defined sites in the cytoplasmic face changed upon formation of Meta II. In addition, some of the interhelical constraints were changed as well. For example, some close contacts between helices are preserved into the Meta II state and some are not.

In Meta II, the retinal conformation is all-trans. The retinal orientation is based on solid-state NMR studies (*35*, *36*) and on photoactivated cross-linking of the β-ionone ring of retinal to the protein (*37*).

A simulated annealing protocol was used to refold the starting structure into a structure that was consistent with the experimental distance constraints characterizing Meta II. Using molecular dynamics within Sybyl, the construct with the distance constraints for Meta II was heated to 1000 °K for 1000 fs and then cooled for 1500 fs to 200 °K. The MMFF94 force field and charges were used within Sybyl. These calculations were performed on a Silicon Graphics R10000 computer.

Molecular Dynamics. The structure of Meta II from Figure 1 was minimized using 4000 steps of ABNR (*38*) minimization. The program CHARMM (*39*, *40*) within INSIGHTII 2000 (Accelrys, San Diego, CA) was used on an Octane R10000 containing processors with MIPS R10010 FPUs. The CHARMM parameter set was used for all protein residues. All minimization and simulations employed a switch nonbond smoothing with a nonbonded cutoff of 14.0 A and dielectric equal to 1.0. Harmonic constraints were applied on the backbone ($k = 25.0$) and fixed constraint on the retinal to preserve the orientation and geometry obtained from NMR experiments. An NVT molecular dynamics simulation was

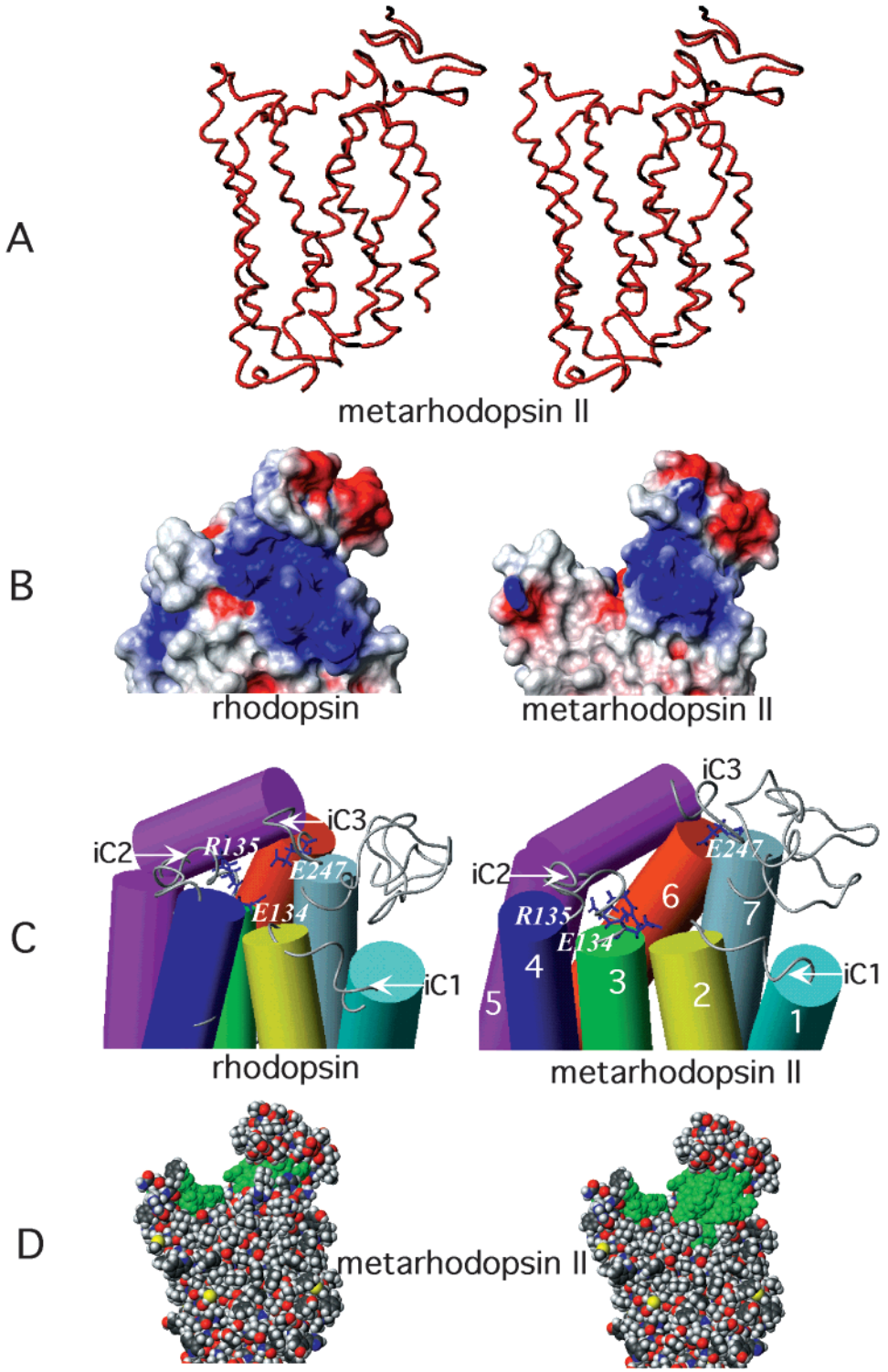

FIGURE 1: Three-dimensional structure of metarhodopsin II determined as described in the text, using previously published methods (*25*). A structure consistent with all the available experimental distance constraints for Meta II results. The cytoplasmic face of the protein is defined by a higher density of experimental distance constraints than the transmembrane domain for Meta II. (A) Stereoview of the backbone of metarhodopsin II. The amino terminus is not included as there are no experimental long-range distance constraints to define the location of that portion of the molecule in the Meta II form. (B) Surface potential, with blue positive and red negative, showing the groove that opens upon formation of meta II (see text). (C) Side view of the cytoplasmic face of rhodopsin and Meta II, with the transmembrane helices color-coded and numbered, showing structural differences between the ground state and excited state of the receptor. The figure shows the clustering of R135, E134, and E247 in rhodopsin and the removal of E247 from the cluster in Meta II. (D) On the left, mapping, in green, of the sequences from rhodopsin peptides (*50*, *51*) that inhibit the interaction between rhodopsin and the G protein, transducin. On the right, addition to the mapping in green of the sequence from the study in Figure 3 (see text). Graphics prepared using Sybyl (Tripos) and MOLMOL (*65*). (PDB entry 1LN6).

done using the Verlet integrator. The system was heated to 300 °K for 10 ps followed by 50 ps equilibration. A 100 ps molecular dynamics simulation was first performed. Temperature and energy stability was checked, and simulation

was continued to 200 ps. For the first 100 ps, energy stabilized at a later part of the simulation. However, energy was stable throughout the next 100 ps.

Phosphodiesterase Activity. PDEase activity was measured as described previously (*27*), measuring hydrogen ion release (*41*). Activity is presented as a percent of control activity with no peptide. Each measurement was performed in triplicate, and the average was calculated.

RESULTS AND DISCUSSION

The medium-resolution structure of Meta II that results from the structure determination method used (Experimental Methods) is shown in Figure 1A. This structure is determined by the experimental distance constraints, both short- and long-range, described above. The result shows a different spatial organization of the helices and turns than exhibited in the ground state rhodopsin structure. These changes occurred in the simulated annealing because of the differences in the experimental long-range distance constraints between those derived from rhodopsin and those derived from Meta II. These changes are indicative of the ability of the experimental long-range distance constraints, obtained from intact protein, to drive the organization of the secondary structure elements into a form that approximates the intact protein (as seen previously for bacteriorhodopsin and rhodopsin). However, the simulated annealing did not alter the start and stop points of helices nor which residues defined the turns, a result of the initial assumption that secondary structure did not change between rhodopsin (ground state) and Meta II. The validity of this assumption was addressed in Experimental Methods.

More experimental long-range distance constraints are available for the cytoplasmic face than for other parts of the structure. Therefore, the organization of this region is better defined than other regions of the protein. The structure indicates that upon conversion of ground state rhodopsin to Meta II, the second and third cytoplasmic loops move apart and change their conformation (the angles these loops form with the protein surface). These conformational changes in cytoplasmic loops two and three open a groove in the surface of the receptor. This groove is partially occluded in ground state rhodopsin. Figure 1B shows a potential surface of the structure of the cytoplasmic face in Meta II relative to ground state rhodopsin. The potential surface within the groove is basic. For example, residues Q236, K245, K311, R314 line one side of this groove and are partly occluded in ground state rhodopsin and fully exposed in Meta II. Other residues, in the first cytoplasmic loop, such as K66, K67, and R69, form the floor of a continuation of the groove, and are exposed in both forms of the protein.

Interestingly, an amphipathic pocket becomes exposed in Meta II. This pocket descends from the surface of the groove (just described) in a location central to all four segments of the cytoplasmic face: iC loops one, two, and three and the carboxy terminus. The pocket is lined by L72 (first cytoplasmic loop), V137, V138 (second cytoplasmic loop), V250, M253, M257 (third cytoplasmic loop), and I307 (carboxyl terminus), but also contains, on one side, E134 and R135 of the highly conserved ERY sequence (see below for more detail).

The structure of Meta II explains some previously published experiments that concern the cytoplasmic face of this receptor. First, the alteration in cytoplasmic loops two and three may have been detected previously. These loops contain β-turns (*20*), and previous FTIR data suggest a change in β-turns in the conformation change from rhodopsin to metarhodopsin II (*31*). Second, both the crystal structure and the NMR structure of rhodopsin (*1*, *26*) show interactions between R135 and E134 and E247 (these interactions are not used as distance constraints in our structural studies). The structure of Meta II shows that upon activation of rhodopsin, the interaction between R135 and E247 is broken due to the conformational change seen in Figure 1C. This disruption of interactions between R135 and E247 was predicted previously for the corresponding residues in other receptors in the same GPCR family. These ionic interactions were hypothesized to stabilize the ground state of the receptor (*42*, *43*).

The transmembrane region of Meta II is defined by fewer experimental long-range distance constraints than are available for rhodopsin (ground state). However, the arrangement of much of the helical bundle is locked by recent experimental data (*44*). These data indicate that the arrangement of helices 1, 2, 5, and 7 is not changed upon conversion of rhodopsin to Meta II. However, helices 3, 4, and 6 move relative to their positions in the rhodopsin structure, and alter in particular the positions of the helices in the cytoplasmic face of the receptor. Specifically, during the photoactivation and the cis−trans isomerization of retinal chromophore, helix 3 is forced outward probably as a result of the steric interaction between C9 methyl group of the chromophore and residues on helix 3. Within the constraints imposed by the work of Oprian (*44*), an inward movement of helix 4 occurs in concert with the outward movement of helix 3. During this cooperative rearrangement, helix 4 is rotated, with A169 coming in close range to the retinal β-ionone ring. According to Baldwin: "All of the helices except IV have some polar-accommodating site in the middle of the most hydrophobic region" (*45*). Therefore, helix 4 does not have a side restricted to interaction with other members of the helical bundle by the polarity and can presumably rotate with minimal cost in energy.

This helical arrangement is consistent with predictions from published work. For example, the movement of helices 3 and 4 allows a contact in Meta II between the β-ionone ring of the retinal and A169 of helix 4 as described previously (*37*). Research conducted with ring-constrained retinal analogues suggests that the retinal undergoes a twist when photoisomerization takes place, which would force a change in orientation of the β-ionone ring (*46*). The β-ionone ring contacts helix 3, and thus a change in the orientation of this ring could induce an alteration in the organization of the transmembrane helices. Those authors suggest initially a movement of helix 3. Such a movement was predicted previously to disrupt restraining interactions that stabilize the ground state of another receptor in the same family (*47*). Helix 6 also moves in this structure of Meta II compared to ground state rhodopsin, and the distance between the cytoplasmic ends of helix 3 and helix 6 increases, as suggested previously (*29*, *48*). Consequently, the cross sectional area of the molecule on the cytoplasmic side increases modestly in the structure of Meta II compared to ground-state rhodopsin, consistent with an expansion of the receptor upon activation (*49*).

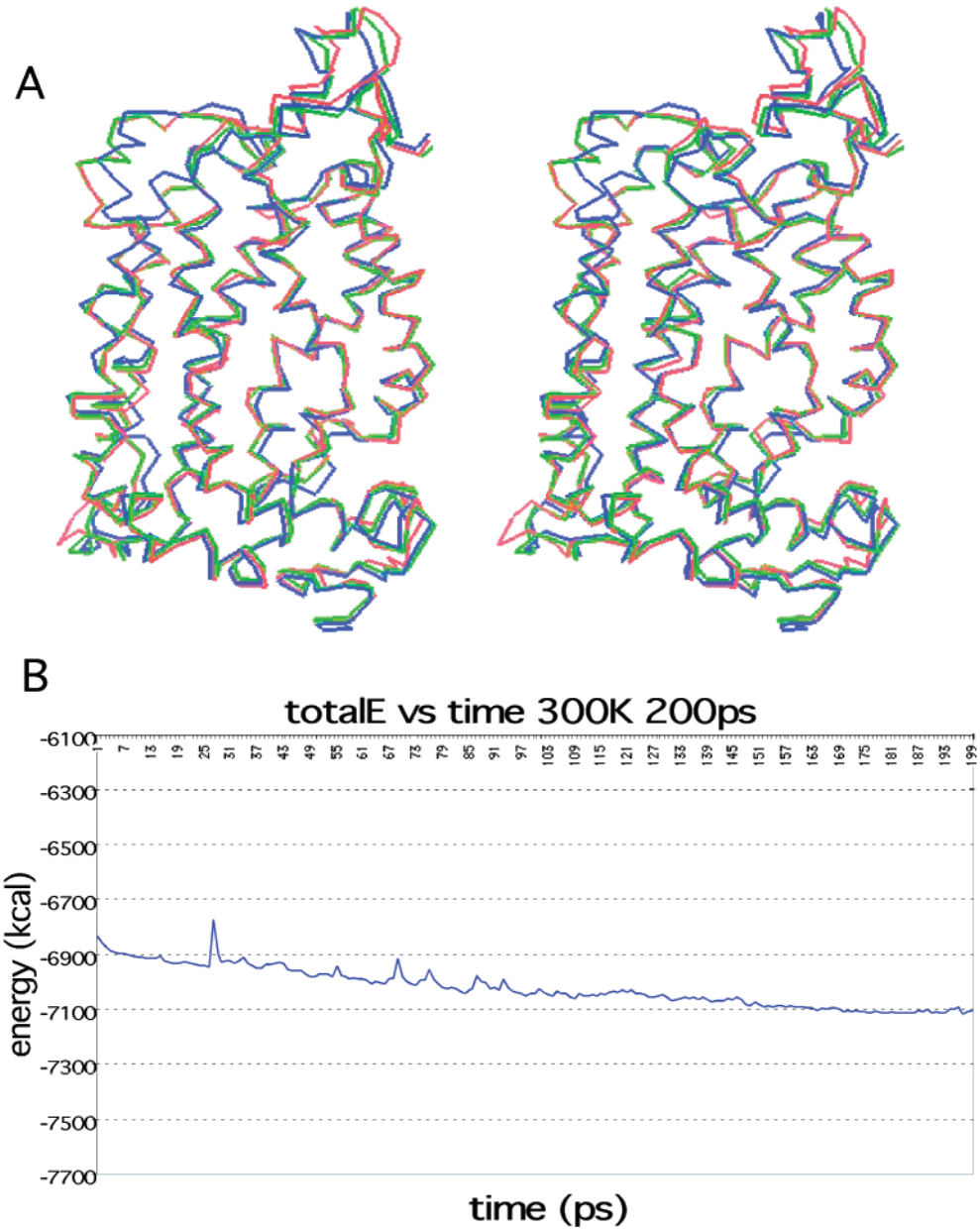

FIGURE 2: Molecular dynamics on Meta II, performed as described in Experimental Methods. The protein was stable throughout the process. Temperature was stable over the 200 ps simulation. The three structures at 0, 100, and 200 ps are superimposed in A in stereo. B is a plot of potential energy vs time for all 200 ps of the molecular dynamics calculation.

An important question with structures determined as we describe in this report is the energetic stability of the structure. If the structure is inherently unstable, then the result is likely not reliable. Therefore, this structure of Meta II was subjected to a stability test using molecular dynamics (Figure 2). The RMSD of the backbone structures between 0 and 100 ps of molecular dynamics is 1.53, and the RMSD between 100 and 200 ps is 1.10. A superposition of the three structures at 0, 100, and 200 ps is presented in Figure 2. These computational results demonstrate that the Meta II structure described herein is energetically stable.

The G-protein, transducin, binds to the cytoplasmic surface of Meta II, but the precise surface for docking is not known. The likely binding site for transducin can now be mapped on the cytoplasmic face of Meta II using sequences of peptides that inhibit the interaction between the receptor and transducin (*50*−*52*). This mapping suggests contact between the G-protein and the groove on the surface of the receptor that is opened upon the formation of Meta II. This surface is shown in Figure 1D.

Although part of this groove is formed by the first cytoplasmic loop of rhodopsin, earlier work (*50*) indicated that this loop was a poor inhibitor of transducin activation by the receptor. The mapping of the binding site in Figure 1D (left) without loop 1 suggests contact between transducin and receptor at the back and along the side of the groove, but misses the base and the front of the groove. Inspection of the Meta II structure indicates that some of the amino acid residues from the first cytoplasmic loop that form the base and front of the groove are not included in the sequences of the peptides from the previous inhibition studies (*50*). Thus, the Meta II structure predicts that an extension of the first cytoplasmic loop on the carboxyl side would yield a more effective inhibitor. A peptide was designed to include

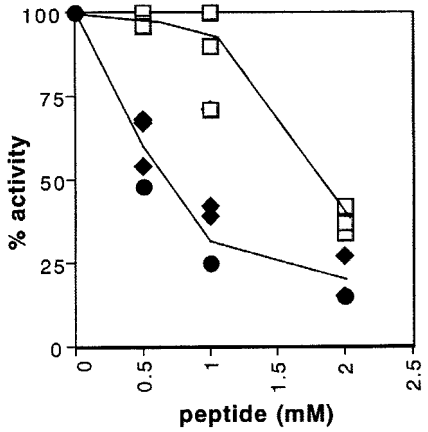

FIGURE 3: Peptide inhibition of phosphodiesterase activation by rhodopsin. Peptides from the first cytoplasmic loop of rhodopsin was tested for ability to inhibit light-stimulated phosphodiesterase (PDEase) activity (which results from transducin binding and activation by Meta II and subsequent activation of PDEase by the transducin α subunit). Two peptides were synthesized from the sequence known from the structure to be in the first cytoplasmic loop: YVTVQHKKLRTPLNYIL (residues 60−76) (rho1), and QHKKLRTPLNYILLNLAVADL (residues 64−84) (rho1c). Rho1 (open symbols) shows poor inhibitory characteristics, in agreement with previous studies on nearly an identical peptide (*50*, *51*). Rho1c (closed symbols) shows 50% inhibition at about one-third the concentration of rho1. The solid diamonds and the solid circles represent two independent experiments performed at different times.

these residues and was tested for its ability to inhibit the cGMP cascade, assayed as previously described (*27*). The longer peptide inhibits the cGMP cascade more effectively than the shorter version of the cytoplasmic loop 1 peptide (Figure 3). Mapping this additional sequence onto the Meta II surface leads to the picture given in Figure 1D (right). This analysis suggests that the entire groove on the cytoplasmic face of Meta II may be involved in binding transducin.

Much work has been reported by many investigators attempting to better define the binding of the G-protein to the receptor. Perhaps the most specific recent work is that reporting chemical cross-links between sites on the receptor and sites on transducin that occur in the complex between transducin and Meta II (*53*, *54*). These studies show that in the complex, the N- and C-termini of transducin α are near the third cytoplasmic loop of Meta II. These cross-linking data and the structure of Meta II suggest that the acidic portion of the amino terminal helix of transducin α (see GRASP picture of transducin (*55*)) may lie in part of the basic groove on the receptor when the G-protein is bound to Meta II and the carboxyl terminal of transducin α may locate in the amphipathic pocket in the bottom of the groove.

REFERENCES

1. Palczewski, K., Kumasaka, T., Hori, T., Behnke, C. A., Motoshima, H., Fox, B. A., Le Trong, I., Teller, D. C., Okada, T., Stenkamp, R. E., Yamamoto, M., and Miyano, M. (2000) *Science 289*, 739−45.
2. Niu, S.-L., Mitchell, D. C., and Litman, B. J. (2001) *J. Biol. Chem. 276*, 42807−42811.
3. Vogel, R., and Siebert, F. (2001) *J. Biol. Chem. 276*, 38487−38493.
4. Popot, J.-L., and Engelman, D. M. (2000) *Annu. Rev. Biochem. 69*, 881−922.
5. Lemmon, M. A., Flanagan, J. M., Hunt, J. F., Adair, B. D., Bormann, B.-J., Dempsey, C. E., and Engelman, D. M. (1992) *J. Biol. Chem. 267*, 7693−7689.
6. Hunt, J. F., Earnest, T. N., Bousche, O., Kalghatgi, K., Reilly, K., Horvath, C., Rothschild, K. J., and Engelman, D. M. (1997) *Biochemistry 36*, 15156−76.
7. Berlose, J., Convert, O., Brunissen, A., Chassaing, G., and Lavielle, S. (1994) *FEBS Lett. 225*, 827−843.
8. Lomize, A. L., Pervushin, K. V., and Arseniev, A. S. (1992) *J. Biomol. NMR 2*, 361−72.
9. Barsukov, I. L., Nolde, D. E., Lomize, A. L., and Arseniev, A. S. (1992) *Eur. J. Biochem. 206*, 665−72.
10. Pervushin, K. V., Orekhov, V. Y., Popov, A. I., Musina, L. Y., and Arseniev, A. S. (1994) *Eur. J. Biochem. 219*, 571−83.
11. Chopra, A., Yeagle, P. L., Alderfer, J. A., and Albert, A. (2000) *Biochim. Biophys. Acta 1463*, 1−5.
12. Yeagle, P. L., Danis, C., Choi, G., Alderfer, J. L., and Albert, A. D. (2000) Molecular Vision www.molvis.org/molvis/v6/a17/.
13. Arshava, B., Liu, S. F., Jiang, H., Breslav, M., Becker, J. M., and Naider, F. (1998) *Biopolymers 46*, 343−357.
14. Gargaro, A. R., Bloomberg, G. B., Dempsey, C. E., Murray, M., and Tanner, M. J. (1994) *Eur. J. Biochem. 221*, 445−54.
15. Piserchio, A., Bisello, A., Rosenblatt, M., Chorev, M., and Mierke, D. F. (2000) *Biochemistry 39*, 8153−60.
16. Xie, H. B., Ding, F. X., Schreiber, D., Eng, G., Liu, S. F., Arshava, B., Arevalo, E., Becker, J. M., and Naider, F. (2000) *Biochemistry 39*, 15462−15474.
17. Franzoni, L., Nicastro, G., Pertinhez, T. A., Oliveira, E., Nakaie, C. R., Paiva, A. C., Schreier, S., and Spisni, A. (1999) *J. Biol. Chem. 274*, 227−35.
18. Katragadda, M., Alderfer, J. L., and Yeagle, P. L. (2000) *Biochim. Biophys. Acta 1466*, 1−6.
19. Mierke, D. F., Royo, M., Pelligrini, M., Sun, H., and Chorev, M. (1996) *J. Am. Chem. Soc. 118*, 8998−9004.
20. Yeagle, P. L., Alderfer, J. L., and Albert, A. D. (1997) *Biochemistry 36*, 3864−3869.
21. Yeagle, P. L., Salloum, A., Chopra, A., Bhawsar, N., Ali, L., Kuzmanovski, G., Alderfer, J. L., and Albert, A. D. (2000) *J. Pept. Res. 55*, 455−465.
22. Jung, H., Windhaber, R., Palm, D., and Schnackerz, K. D. (1995) *FEBS Lett. 358*, 133−6.
23. Abdulaev, N. G., Ngo, T., Chen, R., Lu, Z., and Ridge, K. D. (2000) *J. Biol. Chem. 275*, 39354−39363.
24. Gelber, E. I., Kroeze, W. K., Willins, D. L., Gray, J. A., Sinar, C. A., Hyde, E. G., Gurevich, V., Benovic, J., and Roth, B. L. (1999) *J. Neurochem. 72*, 2206−2214.
25. Katragadda, M., Alderfer, J. L., and Yeagle, P. L. (2001) *Biophys. J. 81*, 1029−1036.
26. Yeagle, P. L., Choi, G., and Albert, A. D. (2001) *Biochemistry 40*, 11932−11937.
27. Yeagle, P. L., Alderfer, J. L., and Albert, A. D. (1995) *Nat. Struct. Biol. 2*, 832−834.
28. Katragadda, M., Chopra, A., Bennett, M., Alderfer, J. L., Yeagle, P. L., and Albert, A. D. (2001) *J. Pept. Res. 58*, 79−89.
29. Farrens, D. L., Altenbach, C., Yang, K., Hubbell, W. L., and Khorana, H. G. (1996) *Science 274*, 768−770.
30. Albert, A. L., B. J. (1978) *Biochemistry 17*, 3893−3900.
31. DeGrip, W. J., Gray, D., Gillespie, J., Bovee, P. H. M., Van den Berg, L. J., and Rothschild, K. J. (1988) *Photochem. Photobiol. 48*, 497−504.
32. Perozo, E., Cortes, D. M., and Cuello, L. G. (1999) *Science 285*, 73−78.
33. Hennessey, J. P. J., and Scarborough, G. A. (1988) *J. Biol. Chem. 263*, 3123−3130.
34. Goormaghtigh, E., Vigneron, L., Scarborough, G. A., and Ruysschaert, J.-M. (1994) *J. Biol. Chem. 269*, 27409−27413.
35. Grobner, G., Burnett, I. J., Glaubitz, C., Choi, G., Mason, A. J., and Watts, A. (2000) *Nature 405*, 810−3.
36. Verdegem, P., Bovee_Geurts, P., Grip, W. d., Lugtenburg, J., and Groot, H. d. (1999) *Biochemistry 38*, 11316−11324.

37. Borhan, B., Souto, M. L., Imai, H., Shichida, Y., and Nakanishi, K. (2000) *Science 288*, 2209−12.
38. Derreumaux, P., Zhang, G., Schlick, T., and Brooks, B. (1994) *J. Comput. Chem. 15*, 532−52.
39. Brooks, B. R., Bruccoleri, R. E., Olafson, B. D., States, D. J., Swaminathan, S., and Karplus, M. (1983) *J. Comput. Chem. 4*, 187−217.
40. MacKerell, A. D., Jr., Bashford, D., Bellott, M., Dunbrack, R. L., Evanseck, J. D., Field, M. J., Fischer, S., Gao, J., Guo, H., Ha, S., Joseph-McCarthy, D., Kuchnir, L., Kuczera, K., Lau, F. T. K., Mattos, C., Michnick, S., Ngo, T., Nguyen, D. T., Prodhom, B., Reiher, W. E., III, Roux, B., Schlenkrich, M., Smith, J. C., Stote, R., Straub, J., Watanabe, M., Wiorkiewicz-Kuczera, J., Yin, D., and Karplus, M. (1998) *J. Phys. Chem. B 102*, 3586−3616.
41. Liebman, P. A., and Evanczuk, A. T. (1982) *Methods Enzymol. 81*, 532−542.
42. Ballesteros, J. A., Jensen, A. D., Liapakis, G., Rasmussen, S. G. F., Shi, L., Gether, U., and Javitch, J. A. (2001) *J. Biol. Chem. 276*, 29171−29177.
43. Shapiro, D. A., Kristiansen, K., Weiner, D. M., Kroeze, W. K., and Roth, B. L. (2002) *J. Biol. Chem. 277*, 11441−11449.
44. Struthers, M., Yu, H., and Oprian, D. D. (2000) *Biochemistry 39*, 7938−42.
45. Baldwin, J. M. (1993) *EMBO J. 12*, 1693−1703.
46. Jang, G.-F., Kuksa, V., Filipek, S., Bartl, F., Ritter, E., Gelb, M. H., Hofmann, K. P., and Palczewski, K. (2001) *J. Biol. Chem. 276*, 26148−26153.
47. Hulme, E. C., Lu, Z.-L., Ward, S. D. C., Allman, K., and Curtis, C. A. M. (1999) *Eur. J. Pharm. 375*, 247−260.
48. Dunham, T. D., and Farrens, D. L. (1999) *J. Biol. Chem. 274*, 1683−1690.
49. Lamola, A. A., Yamane, T., and Zipp, A. (1974) *Biochemistry 13*, 738−745.
50. Konig, B., Arendt, A., McDowell, J. H., Kahlert, M., Hargrave, P. A., and Hofmann, K. P. (1989) *Proc. Natl. Acad. Sci. U.S.A. 86*, 6878−6882.
51. Marin, E. P., Krishna, A. G., Zvyaga, T. A., Isele, J., Siebert, F., and Sakmar, T. P. (2000) *J. Biol. Chem. 275*, 1930−1936.
52. Ernst, O. P., Meyer, C. K., Marin, E. P., Henklein, P., Fu, W.-Y., Sakmar, T. P., and Hofmann, K. P. (2000) *J. Biol. Chem. 275*, 1937−1943.
53. Cai, K., Itoh, Y., and Khorana, H. B. (2001) *Proc. Natl. Acad. Sci. U.S.A. 98*, 4877−4882.
54. Itoh, Y., Cai, K., and Khorana, H. B. (2001) *Proc. Natl. Acad. Sci. U.S.A. 98*, 4883−4887.
55. Lambright, D. G., Sonked, J., Bohm, A., Skiba, N. P., Hamm, H. E., and Sigler, P. B. (1996) *Nature 379*, 311−319.
56. Yang, K., Farrens, D. L., Altenbach, C., Farahbakhsh, Z. T., Hubbell, W. L., and Khorana, H. G. (1996) *Biochemistry 35*, 14040−14046.
57. Gelasco, A., Crouch, R. K., and Knapp, D. R. (2000) *Biochemistry 39*, 4907−4914.
58. Albert, A. D., Watts, A., Spooner, P., Groebner, G., Young, J., and Yeagle, P. L. (1997) *Biochim. Biophys. Acta 1328*, 74−82.
59. Yu, H., Kono, M., McKee, T. D., and Oprian, D. D. (1995) *Biochemistry 34*, 14963−14969.
60. Sheikh, S. P., Zvyaga, T. A., Lichtarge, O., Sakmar, T. P., and Bourne, H. R. (1996) *Nature 383*, 347−350.
61. Yu, H., Kono, M., and Oprian, D. D. (1999) *Biochemistry 38*, 12028−12032.
62. Cai, K., J.Klein-Seetharaman, Hwa, J., Hubbell, W. L., and Khorana, H. G. (1999) *Biochemistry 38*, 12893−12898.
63. Cai, K., Langen, R., Hubbell, W. L., and Khorana, H. G. (1997) *Proc. Natl. Acad. Sci. U.S.A. 94*, 14267−14272.
64. Baldwin, J. M., Schertler, G. F. X., and Unger, V. M. (1997) *J. Mol. Biol. 272*, 144−164.
65. Koradi, R., Billeter, M., and Wuthrich, K. (1996) *J. Mol. Graphics 14*, 51−55.

BI025507W